Optimum Operating Conditions in Ethanol Steam Reforming over a Ni/La_2O_3-αAl_2O_3 catalyst in a Fluidized Bed Reactor

Carolina Montero[a], Aingeru Remiro[b], Pedro Luis Benito[c], Javier Bilbao[b], Ana G. Gayubo[b]*

[a] *Chemical Engineering Faculty, Central University of Ecuador, Ciudad Universitaria-Ritter s/n y Bolivia. Quito, Ecuador. Phone: +593 22544631. Fax: +593 22529676*

[b] *Chemical Engineering Department, University of the Basque Country, P.O. Box 644, 48080. Bilbao, Spain. Phone: +34 946 015361. Fax: +34 946 013 500*

[c] *Mining and Metallurgical Engineering and Materials Science Department, University of the Basque Country, C/ Nieves Cano 12, 01006 Vitoria-Gasteiz, Spain. Phone: +34 945 01 3296.*

*email: carodrmontero@gmail.com

Abstract

This manuscript analyzes the steam reforming of ethanol (SRE) over Ni/La_2O_3-αAl_2O_3 catalyst in a fluidized bed reactor under a wide range of operating conditions (500-650 ºC, space time up to 0.35 $g_{catalyst}h/g_{EtOH}$, and steam/ethanol (S/E) molar ratio in the feed between 3 and 9) in order to select optimum conditions for maximizing H_2 production. The significance the individual reactions in the reaction mechanism have on products distribution and the role of the catalyst in the extent of these reactions have also been analyzed. Blank runs (without catalyst) have been performed to test the contribution of thermal routes to this mechanism. Ethylene and acetaldehyde are intermediate products in the kinetic scheme, whose presence is only observed when ethanol conversion is not complete. The increase in temperature enhances the reforming and decomposition of ethanol and acetaldehyde and, when the catalyst is used, CH_4 reforming and reverse WGS reactions are also promoted, so that the yield of H_2 and CO increases, that of CH_4 decreases and the one of CO_2 remains almost constant with temperature. The increase in S/E molar ratio increases H_2 yield, but attenuates the rate of some reactions involved in the process. 600 ºC, a space time of 0.35 $g_{catalyst}h/g_{EtOH}$ and S/E =6 are suitable conditions for maximizing ethanol conversion (100%) and H_2 yield (82%) with high catalyst stability.

Keywords: ethanol; hydrogen production; steam reforming; fluidized reactor

INTRODUCTION

The foreseen 30 % growth in worldwide energy demand for 2040, together with the increasing social awareness concerning the negative consequences of the use of fossil fuels, has boosted the development of technologies for maximizing energy production from renewable sources, so that 37% of power generation will be from renewable resources in 2040, compared to 23% today [**1**]. Among these, biorefinery technologies aimed at converting different biomass types into chemicals and fuels have a relevant role [2], and the reforming of biomass derived oxygenates has gained an important strategic interest because of the increasing demand of H_2 for use as a fuel, and as raw material in petrochemical industry and agrochemistry [3].

Among biomass derived oxygenates, bio-ethanol has great interest as raw material for producing H_2 by reforming [**4,5**], mainly due to the good perspectives for its production from lignocellulosic biomass, with a forecasted increase from the current 270 L/tonne biomass to 400 L/tonne biomass in 2030, as a result of the advance in the technology of enzymatic hydrolysis-fermentation [**6**]. Moreover, the steam reforming (SR) of bio-ethanol (~86 % H_2O) avoids the high cost required for its dehydration (estimated at 50 % the total product cost [**7**]) in order to be used as a fuel (dehydrated ethanol).

The steam reforming of ethanol (SRE) is an endothermic process that proceeds at relatively low temperatures (between 300 and 800 ºC), with the following stoichiometry:

$$C_2H_5OH + 3H_2O \rightarrow 6H_2 + 2CO_2 \qquad \Delta H^0_{298} = 173.3 \text{ kJ/mol} \qquad (1)$$

The use of steam/ethanol (S/E) molar ratio in the feed above the stoichiometric value (S/E = 3) improves H_2 selectivity and attenuates deactivation by coke deposition [**8**]. Nevertheless, the reaction mechanism is complex due to secondary reactions that take place in parallel to steam reforming reaction and generate intermediate products and by-products, thus reducing H_2 yield. Among the secondary reactions, the following are considered **[9-11]:**

Ethanol dehydrogenation: $C_2H_5OH \leftrightarrow C_2H_4O + H_2$ (2)

Ethanol dehydration: $C_2H_5OH \rightarrow C_2H_4 + H_2O$ (3)

Ethanol decomposition: $C_2H_5OH \rightarrow H_2 + CO + CH_4$ (4)

Acetic acid formation: $C_2H_5OH + H_2O \rightarrow CH_3COOH + 2H_2$ (5)

Acetone formation: $2\ C_2H_5OH \rightarrow CH_3COCH_3 + CO + H_2$ (6)

Acetone steam reforming: $CH_3COCH_3 + 2H_2O \rightarrow 3CO + 5H_2$ (7)

Acetic acid steam reforming: $CH_3COOH + 2H_2O \rightarrow 2CO_2 + 4H_2$ (8)

Incomplete ethanol reforming:	$C_2H_5OH + H_2O \rightarrow CH_4 + 2H_2 + CO_2$	(9)
Acetaldehyde decomposition:	$C_2H_4O \rightarrow CH_4 + CO$	(10)
Acetaldehyde reforming:	$C_2H_4O+H_2O \rightarrow 2CO+3H_2$	(11)
	$C_2H_4O + 3H_2O \rightarrow 2CO_2 + 5H_2$	(12)
Water Gas Shift reaction:	$CO + H_2O \leftrightarrow H_2 + CO_2$	(13)
Methane steam reforming (reverse to methanation of CO and CO_2):	$CH_4 + H_2O \leftrightarrow CO + 3H_2$	(14)
	$CH_4 + 2H_2O \leftrightarrow CO_2 + 4H_2$	(15)
Ethylene steam reforming:	$C_2H_4 + 2H_2O \rightarrow 4H_2 + 2CO$	(16)

Other reactions take also place, which are not relevant for products distribution, but they contribute to catalyst deactivation by formation or elimination (by gasification) of coke (C):

Ethylene polymerization:	$C_2H_4 \rightarrow$ polymers $\rightarrow C$	(17)
Boudouard reaction:	$2CO \leftrightarrow C + CO_2$	(18)
Methane decomposition:	$CH_4 \rightarrow 2H_2 + C$	(19)
Coke gasification:	$C + H_2O \rightarrow CO + H_2$	(20)

Due to the complexity of the reaction scheme, the yield and selectivity of H_2 is highly affected by reaction conditions (temperature, S/E molar ratio, space time), as well as by catalyst composition. Consequently, the industrial viability of SRE process requires the development of catalysts that are highly active and selective for H_2 formation (thus minimizing secondary reactions), which are stable and hardly affected by coke formation. With this objective, several reviews have analyzed the use of catalysts with both noble and non-noble metals, supported on different oxides [**9,12-15**]. Noble metal catalysts, especially Rh based catalysts, are highly active and selective for SRE [**16,17**], but their practical applications are limited by their high cost. Among the non-noble catalysts, those based on Ni and Co are the most studied due to their high C-C- bond breakage activity [**18-23**].

Furthermore, it is well established that an increase in metal content in Ni based catalysts improves ethanol conversion, but it does not guarantee a higher H_2 selectivity. Thus, Han et al. [**24**] determined an optimum content of 15 wt% Ni for a catalyst prepared by sol-gel technique, which showed a high Ni dispersion and resistance to coke deposition. Gayubo et al. [**25**] reported an optimum content of 10 wt% Ni in Ni/SiO_2 and Ni/α-Al_2O_3 catalysts prepared by incipient wetness impregnation, which is due to a higher Ni content leading to a significant agglomeration of metal crystals.

γ-Al_2O_3 has been widely used as support because of its high thermal and mechanical stability, linked to its high specific surface area, which also improves the dispersion of the active phase. Nevertheless, its acidity promotes ethanol dehydration reaction and, as a result, coke deposition via ethylene, which causes a rapid deactivation of the catalyst. Consequently, several methods have been studied for the neutralization of its acidity. The addition of basic additives, such as CaO, lowers the support acidity and also weakens the interaction between Ni and Al_2O_3, which facilitates the reduction of Ni^{+2} species to Ni^0 **[26,27]**. However, Ca contents above 5 wt% increase Ni active particle size, which causes a lower H_2 yield [**27**] and promotes the formation of encapsulating coke responsible for the rapid deactivation of the catalyst [**26**]. The addition of MgO to γ-Al_2O_3 caused similar results to those obtained by doping with CaO [**28-30**]. Nevertheless, the doping of the support ZrO_2 with CaO did not affect Ni reducibility and inhibited coke deposition [**31**]. Furthermore, the addition of La_2O_3 provides stability to Ni/Al_2O_3 catalyst by lowering coke formation rate [**32-34**]. In a previous work, a Ni/La_2O_3-αAl_2O_3 catalyst used in the SRE reaction achieved an equilibration state subsequent to a reaction-regeneration cycle (consisting in the steam reforming at 700 ºC followed by coke combustion with air at 550 ºC), which allowed attaining a reproducible performance in successive reaction-regeneration cycles [**35**].

In view of this background, this work analyzes the effect operating conditions (temperature, S/E molar ratio, space time) have on the behavior of an equilibrated Ni/La_2O_3-αAl_2O_3 catalyst in the SRE process, in order to determine the conditions maximizing ethanol conversion and H_2 yield. Moreover, the relevance on products distribution of the individual reactions of the complex reaction mechanism (Eqs. 1-16), and the role of catalyst in the extent of these reactions has been also analyzed. With this objective, blank runs (without catalyst) have been performed to test the contribution of thermal routes to the reaction mechanism. Moreover, catalyst stability has been approached by means of long duration runs (200 h), as it is an essential aspect for larger scale applications.

EXPERIMENTAL SECTION

Catalyst preparation

The catalyst was prepared by incipient wetness impregnation method, and with a composition (10 wt% Ni and 9 wt% La_2O_3) determined in a previous work [**36]**. It has been proven that once calcined at 550 ºC for 2 h in air, and subsequent to an equilibration treatment, the catalyst achieves a reproducible kinetic behavior in reaction-regeneration cycles [**35**]. Prior to the kinetic runs the catalyst was reduced in situ at 700 °C for 2 h by using a H_2–He flow (10 vol% H_2). The properties (Table 1) have been determined as follows: composition, by

inductively coupled plasma and atomic electron spectroscopy (ICP-AES) in a Thermo X7-II spectrometer; surface area (S_{BET}) and porous structure, by N_2 adsorption−desorption in a Quantacrome Autosorb IQ2 physisorption mode; metal surface area and dispersion, by H_2 chemisorption in a Quantacrome Autosorb IQ2.

Temperature programmed reduction (TPR) measurements were conducted on an AutoChem II 2920 Micromeritics. The TPR profile of this catalyst showed three reduction peaks [**35]**: i) a peak below 380 ºC, corresponding to the reduction of bulk NiO clusters with low interaction with the support; ii) a main reduction band, in the 400-700 ºC range (which can be decomposed into two peaks), usually ascribed in the literature to the reduction of dispersed NiOx species, which are probably amorphous and interact strongly with the support **[37**], or to the reduction of $LaNiO_3$ [**38**]; iii) a small peak above 700 ºC, corresponding to the $NiAl_2O_4$ spinel, which has probably been formed by migration of Ni atoms on Al_2O_3 [**39**].

The X-ray diffraction (XRD) pattern measured on a Bruker D8 Advance diffractrometer with a CuKα1 radiation showed diffraction lines corresponding to the reflection of Al_2O_3 phase and Ni^0 phase (at 2θ angle of 44.5º, 51.9º and 76.4º). $LaAlO_3$ phase (La_2O_3 combined with α-Al_2O_3) is also detected [**40**].

Table 1

Reaction equipment and experimental conditions

The runs were carried out in automated reaction equipment (Microactivity reference-PID Eng & Tech) provided with an isothermal fluidized bed reactor (22 mm internal diameter and total length of 460 mm), connected on-line to a gas chromatograph (Agilent 3000) provided with four modules for the analysis of products: 1) permanent gases (O_2, N_2, H_2, CO, and CH_4) with 5A molecular sieve capillary column; 2) light oxygenates (C_2−), CO_2 and water, with Plot Q capillary column; 3) C_2-C_4 hydrocarbons, with alumina capillary column; 4) oxygenated compounds (C_{2+}) with Stabilwax type column. The use of a fluidized bed is interesting in order to guarantee the isothermicity of the bed and also attenuate deactivation by coke deposition [33,41].

In order to ensure a correct fluidization of the bed and avoid internal and external diffusional restrictions in the catalyst particles, the following conditions have been established [**41**]: a bed made up of catalyst (particle diameter between 0.15 and 0.25 mm) and inert solid (CSi, 37μm)

in a mass ratio inert:catalyst > 8:1; bed height/bed diameter of 2; gas flow rate at the reactor inlet ~ 7.6 $cm^3\ s^{-1}$, corresponding to a gas linear velocity of 2.4 $cm\ s^{-1}$, which accounts for 6 times the minimum fluidization velocity.

The conditions of the catalytic runs are as follows: temperature between 500 and 650 °C; steam/ethanol molar ratio (S/E) between 3 and 9; space time between 0.02 and 0.35 $g_{catalyst}h/g_{EtOH}$ (with a catalyst mass between 0.03 to 0.525 g); total pressure, 1.4 bar; partial pressure of ethanol, 0.08 bar.

Blank runs (without catalyst) have been performed in order to delimit the temperature from which there is a noticeable contribution of thermal routes to the reaction mechanism. These runs have been carried out with inert solid (CSi) in the fluidized bed, in the 500-700 ºC range, with an S/E molar ratio between 3 and 9, and maintaining the same hydrodynamic conditions than in the runs with catalyst.

Reaction indices

The kinetic behaviour has been quantified by considering the following reaction indices:

Conversion of ethanol (X), which is calculated from its molar flow rate (F) at the inlet and outlet (unreacted ethanol) of the catalytic reactor:

$$X = \frac{F_{inlet} - F_{outlet}}{F_{inlet}} \quad (21)$$

The yield of each product (Y_i) is calculated as the ratio between the molar flow rate of product i (F_i) and the maximum molar flow rate that may be obtained according to stoichiometry when ethanol is fed into the reactor:

$$Y_i = \frac{F_i}{\upsilon_i \cdot F_{inlet}} \quad (22)$$

where $\upsilon_i = 6$ for H_2, $\upsilon_i = 2$ for CO_2, CO and CH_4, and $\upsilon_i = 1$ for acetaldehyde and ethylene.

The selectivity of each gaseous product (S_i) is calculated as the ratio between the molar flow rate of product i (F_i) and the molar flow rate of all the reaction products (ethanol and water excluded):

$$S_i = \frac{F_i}{\sum_i F_i - F_E - F_W} \quad (23)$$

RESULTS AND DISCUSSION

Contribution of thermal routes to SRE mechanism

Figures 1 and 2 show the composition (molar fraction on a water free basis) of the products stream at the reactor outlet obtained in the runs without catalyst at different temperatures and S/E molar ratios. Figure 1 corresponds to ethanol (Figure 1a) and H_2 (Figure 1b), whereas each graph in Figure 2 corresponds to a carbon product (acetaldehyde, ethylene, CO and CH_4). The composition of CO_2 (below 2 % under all the studied conditions) is not shown. Moreover, neither acetone nor acetic acid has been observed in the products stream in the temperature range studied.

It is observed that at 500 ºC ethanol conversion is low and the product stream is mainly composed of ethanol (~95 %), with low concentrations of H_2 (~2.5 %), acetaldehyde (~2.5 %), and ethylene (~0.1 %). Moreover, at this temperature, the results are not affected by S/E molar ratio.

The increase in temperature up to 600 ºC involves a slight increase in ethanol conversion. However, above this temperature ethanol conversion rapidly increases, so that its molar fraction decreases noticeably (Figure 1a) and H_2 molar fraction increases almost linearly, achieving a value of 0.36 at 700 ºC and for S/E =9 (Figure 1b). The molar fractions of carbon products have different trends with temperature (Figure 2). Acetaldehyde is the major product in the 600-650 ºC range (Figure 2a), whereas the formation of CO and CH_4 increases exponentially with temperature above 650 ºC (Figures 2c, 2d), and the formation of CO_2 (not shown) is almost insignificant. These results give evidence that an increase in temperature promotes firstly ethanol dehydrogenation to form acetaldehyde (Eq. 2) (whose presence is significant at 500 ºC), and subsequently ethanol dehydration to form ethylene (Eq. 3) (whose formation is noticeable above 550 ºC), whereas the decomposition of ethanol (Eq. 4) or acetaldehyde (Eq. 10) to produce CO and CH_4 are only significant above 650 ºC, and they are enhanced exponentially with temperature. The similar concentration of CO and CH_4 obtained at high temperature, as well as the almost insignificant formation of CO_2 gives evidence that, in the absence of catalyst, WGS reaction (Eq. 13), methane steam reforming (Eqs. 14 and 15) and direct steam reforming of ethanol (Eq. 1) do not have a significant contribution to the reaction mechanism in the 500-700 ºC temperature range.

Furthermore, an increase in S/E molar ratio has lower effect than temperature on these results. In general, all the thermal routes are promoted by increasing S/E molar ratio from 3 to 6, although a further increase in this variable has no significant effect.

Figure 1

Figure 2

There are scarce papers in the literature reporting results without catalyst in order to analyze the thermal routes for ethanol conversion under steam reforming conditions. The aforementioned results are consistent with those by Fatsikostas and Verykios [**42**] obtained by experimentation at temperature programmed under conditions of SRE reaction (S/E=3 in the 500-800 ºC range). These authors concluded that ethanol conversion is activated from 600 ºC on, and is significant above 700 ºC. At low temperature, ethanol dehydrogenation was the prevailing reaction, whereas at high temperature dehydration and cracking/dissociation were the main reactions. Melchor-Hernández et al. also obtained a significant ethanol conversion above 600 ºC for S/E=3 [**43**]. Barattini et al. [**44**] operated in a fixed bed reactor with quartz as inert solid with S/E=3 and found that ethanol conversion was significant above 430 ºC, and complete at 790 ºC. At low temperature (400 ºC), the main products were ethylene and acetic acid, whereas at higher temperature (730 ºC) small amounts of CO, CH_4 and H_2 were obtained and ethylene selectivity remained stable in the studied temperature range, and acetaldehyde was not detected, differently to the results in this paper and to those by Fatsikostas and Verykios [**42**].

Based on these results, and although the higher reaction rate of the catalyzed steps will minimize the contribution of the thermal routes, the 500-650 ºC range has been selected in order to analyze the effect of operating variables on catalyst performance (next section). This range is wide enough, and minimizes the contribution of thermal routes, so that conclusions concerning activity, selectivity and stability of the catalyst itself can be inferred.

Effect of operating conditions for 10Ni/La_2O_3-αAl_2O_3 catalyst

This section analyzes the effect operating conditions (temperature, space time and S/E molar ratio) have on the reaction indices at zero time on stream, which have been obtained by extrapolating the results obtained in runs of 20 h duration to zero time.

Effect of Temperature

The effect temperature has on the reaction indices is shown in Figures 3 and 4, in which the values are shown for ethanol conversion and H_2 yield (Figure 3), and carbon products yields

(Figure 4). The results correspond to S/E molar ratio of 3 (which is the stoichiometric ratio for SRE reaction) and for two values of space time, low (0.04 $g_{catalyst}h/g_{EtOH}$) and high (0.35 $g_{catalyst}h/g_{EtOH}$), with the aim of establishing the effect of temperature under conditions far from equilibrium (kinetic regime) and close to equilibrium (thermodynamic regime), respectively. It should be pointed out, that neither acetone nor acetic acid is present in the products stream in the experimental conditions studied. The explanation may lie in the fact that the reactions corresponding to their formation/disappearing (Eqs. 5-8) are very rapid or do not occur. In fact, taking into account that these products are not observed in the blank runs either, it can be concluded that the reactions do not occur.

Under kinetic regime (space time of 0.04 $g_{catalyst}h/g_{EtOH,}$ continuous lines), high ethanol conversion (0.6) is obtained at 500 ºC, which progressively increases with temperature and almost full conversion is achieved at 650 ºC (Figure 3). For a high space time (0.35 $g_{catalyst}h/g_{EtOH}$, dashed lines) ethanol conversion is full for the whole temperature range studied. This effect of temperature is consistent with that observed in the literature for different catalysts and reaction conditions **[**43,45-49**].** Thus, according to Fasikostas et al. [45], who used 30%Ni/La_2O_3/Al_2O_3 catalyst, S/E=3 and a space time of 0.29 $g_{catalyst}h/g_{EtOH}$, conversion increases from 0.2 at 600 ºC to 0.92 at 800 ºC, and is full at 850 ºC. Melchor-Hernández et al. [43] used 10%Ni/8%La_2O_3-γAl_2O catalyst prepared by sol-gel method, S/E= 3 and space time ~0.07 $g_{catalyst}h/g_{EtOH}$ and obtained high ethanol conversion from low temperature (0.88 at 450 ºC and 0.94 at 500 ºC) and total conversion at 600 ºC, although their H_2 yield was rather low (0.04 at 400 ºC and 0.50 at 600 ºC). They also proved that this yield was slightly higher for a higher La_2O_3 content in the support. The increase in ethanol conversion with temperature is more pronounced for Llera et al. [46] (from 0.10 to 0.55 in the 600-650 ºC temperature range) when they used Ni/Al_2O_3/LDH catalyst, S/E=5.5 and a low space time, whereas Patel et al. [47] obtained 0.95 conversion at 600 ºC and full at 700 ºC with Ni/Ce_2O_3/Zr_2O_3 catalyst [47], for a high space time and S/E=9. In the steam reforming of bioethanol (14 wt % ethanol) on 10%Ni/6%La_2O_3-Al_2O_3 catalyst, total ethanol conversion was achieved at 350 ºC, which can be partially attributed to the high S/E ratio (~15) [49].

Figure 3

Figure 4

Concerning the H_2 yield obtained in this work (empty symbols in Figure 3), it increases with temperature (from 0.19 at 500 ºC to 0.33 at 650 ºC) under kinetic regime conditions (low space time), although to a lesser extent than ethanol conversion, especially above 600 ºC. Under conditions with full ethanol conversion (high space time), H_2 yield increases with temperature in the 500-650 ºC range (from 0.40 to 0.73), but in a less pronounced way above 600 ºC. It should be mentioned that these results correspond to S/E=3, and that a higher H_2 yield (0.88) was obtained for a higher S/E ratio (S/E=9) at 600 ºC.

This evolution of H_2 yield, which is different to the evolution of ethanol conversion, is explained by the different effect of temperature on the reactions of the overall mechanism (Eqs. 1-16), which also involves a noticeable change in the yields of carbon products with temperature, as shown in Figure 4. Under kinetic regime conditions (low space time, 0.04 $g_{catalyst}h/g_{EtOH}$) (Figure 4a), the order of the yields at 500 ºC is: acetaldehyde (0.24) > CO_2 (0.08) > CO (0.06) > CH_4 (0.05) > C_2H_4 (0.01). It should emphasized that under these conditions, H_2/CO_2 molar ratio (6.91) is noticeably higher than the stoichiometric value (3) corresponding to ethanol reforming reaction (Eq. 1). These results give evidence that at 500 ºC the fastest reaction in the kinetic scheme is the dehydrogenation to acetaldehyde (Eq. 2), which is noticeably faster than ethanol reforming (Eq. 1). However, the latter is faster than the decomposition reactions (of both ethanol and acetaldehyde, Eqs. 4 and 10), and the WGS (Eq. 13), methane reforming (Eqs. 14-15) and dehydration to ethylene (Eq. 3) are apparently slow reactions, specially the last one. When temperature increases above 600 ºC, acetaldehyde yield decreases noticeably, (slightly lower than 0.1 at 650 ºC), whereas the yield of the remaining carbon products increases, especially that of ethylene, with the lower increase corresponding to methane. Consequently, H_2/CO_2 molar ratio decreases asymptotically with temperature (to 5.3 at 650 ºC). These results give evidence that an increase in temperature promotes mainly ethanol dehydration (Eq. 3), as well as ethanol and acetaldehyde decomposition (Eqs. 4 and 10) and the reforming of acetaldehyde (Eqs. 11 and 12) and CH_4 (Eqs. 14-15).

For a high space time value (0.35 $g_{catalyst}h/g_{EtOH}$, Figure 4b), that is, under conditions with total ethanol conversion and close to the thermodynamic equilibrium, there is almost total absence of ethylene in the whole temperature range studied, and acetaldehyde formation is not observed above 550 ºC. This result is consistent with the role of both compounds as intermediate products in the reaction scheme, and therefore their transformation reactions (reforming of ethylene and decomposition/reforming of acetaldehyde) are complete under the

studied conditions. Furthermore, methane yield decreases almost linearly with temperature (from 0.45 at 500 ºC to 0.13 at 650 ºC) and a significant increase in CO yield takes place at the same time (similarly to that obtained for H_2 yield under these conditions, Figure 3), which evidences an important contribution of methane steam reforming reaction (Eq. 14) to the global reaction mechanism at high temperatures (because this reaction is highly endothermic), with a noticeably increase in H_2 yield. The CO_2 yield is high and almost constant (~0.46) in the 500-600 ºC range, and decreases slightly above 600 ºC due to the shift in the thermodynamic equilibrium of the exothermic WGS reaction (enhancing the reverse WGS reaction). The fact that CO_2 yield remains almost constant in the 500-600 ºC range, even though there is an increase in the reaction rate of steam reforming of oxygenates and hydrocarbons, should be attributed to CO_2 consumption in both the methanation reaction (reverse Eq. 15) and the subsequent CH_4 reforming, as well as in the dry reforming of oxygenates and hydrocarbons, as pointed out by Fatsikostas et al. **[45]**.

As previously mentioned, the properties of the support have an important role in products distribution. Thus, Melchor-Hernández et al. (2013) obtained a maximum ethylene yield of ~0.35 in the 500-550 ºC range, with a subsequent decrease to ~ 0.20 at 600 ºC, with the yield being lower for a higher La content in the support [**43**]. This high ethylene yield was a consequence of the slightly acidic support (γ-Al_2O_3), which is highly active for ethanol dehydration reaction. On the contrary, with a Ni/SiO_2 catalyst and under similar conditions to those used in this work, Vicente et al. [**10**] reported total absence of ethylene in the product stream due to the non-acidic SiO_2 support, which minimizes ethylene dehydration reaction. Moreover, with this support without activity for ethanol dehydration, the competence of catalytic reactions with thermal reactions avoided the formation of ethylene even at high temperatures.

Effect of space time

Figure 5 shows the effect of space time on ethanol conversion and H_2 yield for different temperatures, and Figure 6 the effect of space time on the carbon products yields for two temperatures (500 ºC (Figure 6a) and 650 ºC (Figure 6b), which are the limits of the studied range). These results correspond to an S/E molar ratio of 3, and similar trends have been observed for the ratios of 6 and 9.

Ethanol conversion increases in a pronounced way with space time (Figure 5), although more moderately at high temperatures due to the significant contribution of thermal routes to the reaction mechanism. For all the studied temperatures, H_2 yield (empty symbols in Figure 5) increases in a pronounced way with space time in the 0.02-0.09 $g_{catalyst}h/g_{EtOH}$ range. A maximum is achieved for 0.09 $g_{catalyst}h/g_{EtOH}$, when ethanol conversion is complete, and below 550 ºC H_2 yield decreases with an increase in space time due to the relevance of methanation reactions at these temperatures (reverse Eqs. 14-15), and tends towards the thermodynamic equilibrium values [**11**]. Consequently, the yield of CH_4 increases (Figure 6a), although less noticeably as temperature is increased.

Figure 5

Figure 6

Two zones are also identified in the evolution with space time of carbon products yields (Figure 6), similarly to those observed in Figure 5 for ethanol conversion and H_2 yield, although the range in which the effect of space is noticeable depends on temperature: i) at 500 ºC (Figure 6a) there is a noticeable effect of space time on the yields of all carbon products in the 0.02-0.18 $g_{catalyst}h/g_{EtOH}$ range; ii) at 650 ºC (Figure 6b) a significant variation in the products yields takes place below 0.09 $g_{catalyst}/hg_{EtOH}$ (that is, before achieving total ethanol conversion). For both temperatures, acetaldehyde and ethylene are the main products at low space time values, specially the former, which confirms that ethanol dehydrogenation and dehydration reactions, especially the former, are the fastest reactions in the kinetic scheme, which is more noticeable at high temperature for the dehydration reaction. Moreover, CO and CO_2 yields at both temperatures increase sharply for low space time values, and subsequently CO_2 yield continues increasing asymptotically towards the thermodynamic equilibrium value [11], whereas CO yield, which peaks at 0.09 $g_{catalyst}h/g_{EtOH}$, decreases slowly towards the corresponding thermodynamic equilibrium value [11]. A 500 ºC, the increase in CH_4 yield is almost parallel to that of CO_2, and progressively attenuates with the increase in space time (Figure 6a). Furthermore, CH_4 formation is faster at 650 ºC (Figure 6b), thus achieving a significant value at a low space time value, which confirms the importance of thermal routes in ethanol and acetaldehyde decomposition reactions (Eqs. 4 and 10, respectively) at this temperature.

Similar trends in the effect of space time in ethanol conversion and products yield have been observed in literature for other Ni based catalysts, although the range of space time depends on catalyst composition and on the remaining reaction conditions. Thus, Llera et al. ([**46**], obtained a conversion of 0.50 for 0.035 $g_{catalyst}h/g_{EtOH,}$ and total conversion for 0.14 $g_{catalyst}h/g_{EtOH}$, at 650 ºC and S/E=5.5, on a Ni/Al_2O_3/LDH catalyst. According to these authors, H_2 yield increased with space time to 0.80 for 0.14 $g_{catalyst}h/g_{EtOH}$, and decreased slightly for higher space time. With a skeletal (non-supported) Ni-based catalyst Zhang et al. [**48**] obtained total ethanol conversion for a space time above 0.15 $g_{catalyst}h/g_{EtOH}$, whereas H_2 yield remained almost constant (0.60) in the 0.07-0.35 $g_{catalyst}h/g_{EtOH}$ range, at 450 ºC with S/E=8. An increase in ethanol conversion with space time was also observed for Patel et al. [**47**]. on a $Ni/Ce_2O_3/Zr_2O_3$ catalyst, with values of up to 0.95 for 0.60 $g_{catalyst}h/g_{EtOH,}$ at 650 ºC and with S/E=4. According to these authors, H_2 yield varied in the 0.70-0.80 range, which is slightly higher than that shown in Figure 5, probably due to the higher S/E ratio used. For a commercial 15%Ni/Al_2O_3 in the 200-600 ºC range and for S/E=10, two zones were also identified by Wu et al. [**50**] , below and above a certain value of space time (corresponding to a contact time of 1 s). Thus, with an increase in space time, the increase in CO_2 yield is less pronounced in the second zone (> 1 s). Furthermore, CO yield peaks for a space time at 600 ºC, whereas CH_4 yield (higher at low temperature) increased with space time in the first zone (< 1 s), and acetaldehyde yield decreased continuously with space time, especially at 600 ºC.

Effect of steam/ethanol molar ratio

The effect of this variable has been more scarcely studied in literature than that of temperature. Most of the research has been carried out with S/E molar ratio=3, which corresponds to the stoichiometric value [**11-13,51**]. The results with S/E values above 6 correspond to studies on bio-ethanol steam reforming, whose characteristic ethanol content is around 14 wt %, and therefore S/E ratio is of around 15 [**52**].

Figure 7 shows the evolution with S/E molar ratio (in the 3-9 range) of ethanol conversion and H_2 yield at 600 ºC for a space time of 0.18 $g_{catalyst}h/g_{EtOH}$. For this high value of space time ethanol conversion is complete for all the S/E molar ratios studied, but a significant effect of this variable on H_2 yield is observed, as predicted by thermodynamics [**11**]. Thus, H_2 yield increases almost linearly by increasing S/E molar ratio, because the excess of water favours the reactions producing H_2, such as ethanol and methane reforming, and WGS reaction. This effect explains the evolution of products selectivity with S/E molar ratio shown

385 in Figure 8, corresponding to the same temperature and space time as Figure 7. As S/E ratio is
386 increased there is an almost linear increase in the selectivities of H_2 and CO_2, although the
387 latter to a lesser extent, whereas the selectivity of CO and CH_4 progressively decrease, as a
388 consequence of the increase in the rates of WGS and CH_4 reforming reactions.

389 **Figure 7**

390 **Figure 8**

391 Similar trends in carbon products selectivity by changing S/E ratio have been also observed
392 by Carrera-Cerritos et al. [**18**] and Li et al. [**53**]. According to Li et al. [**53**]., an increase in
393 CO_2 yield of the same order as the decrease in CH_4 yield is explained because the WGS
394 reaction is enhanced at the same extent as the CO methanation reaction is hindered.

395 The selectivies of acetaldehyde and ethylene have not been plotted in Figure 8 because their
396 presence has not been detected for this high value of space time. Under conditions they appear
397 in the reaction medium (space time below 0.09 $g_{catalyst}h/g_{EtOH}$), their selectivity decrease with
398 an increase in the S/E molar ratio.

399 In order to complement the previous results, corresponding to total ethanol conversion, the
400 effect of S/E molar ratio on ethanol conversion and H_2 yield has been studied with runs at low
401 values of space time (0.04 $g_{catalyst}h/g_{EtOH}$). As observed in Figure 9, ethanol conversion in the
402 500 -550 ºC range (kinetic regime) is lower as the S/E molar ratio is increased. This result
403 gives evidence that excess of water with respect to the stoichiometric value attenuates the
404 global reaction mechanism for ethanol steam reforming (Eqs. 1-16) due to the lower rate of
405 some of the reactions in the kinetic scheme, such as ethanol dehydrogenation and dehydration,
406 and ethanol and acetaldehyde decomposition. This attenuation should be taken into account in
407 future studies for the development of a kinetic model for this process. In the 500-550 ºC
408 temperature range, H_2 yield is slightly affected by an increase in the S/E molar ratio because
409 the drop in ethanol conversion is balanced by the increase in H_2 selectivity. A similar effect of
410 S/E ratio was observed by Carrera-Cerritos et al. [**18**] on a 10Ni/La_2O_3-Al_2O_3 catalyst used in
411 a fixed-bed reactor, at 600 ºC and a space time of 0.10 $g_{catalyst}h/g_{EtOH}$. These authors obtained
412 complete conversion with S/E=3, whereas for S/E=6 the conversion decreased to 0.89, and H_2
413 yield did not increase with S/E ratio.

Nevertheless, Figure 9 shows that H_2 yield noticeably increases when S/E ratio is increased in the 550-650 ºC range because an increase in S/E molar ratio under these conditions (of high conversion) hardly attenuates ethanol conversion.

Figure 9

Taking into account the above mentioned results concerning the effect of operating conditions on products distribution obtained on a Ni/La_2O_3-Al_2O_3 catalyst, and their explanation based on the relevance of the possible steps in the reaction mechanism (Eqs. 1-16), the kinetic scheme plotted in Figure 10 has been established. This scheme only considers the reactions that affect products distribution in the range of reaction conditions studied, and is useful for quantifying this distribution by means of a kinetic model. In this scheme, continuous arrows denote irreversible reactions, whereas dashed arrows denote reversible reactions. Blue arrows indicate the reactions that are favored by an increase in S/E molar ratio (enhancing H_2 production), whereas black arrows denote reactions attenuated by increasing S/E molar ratio (decreasing ethanol conversion).

Figure 10

Catalyst stability

In order to test the stability of the catalyst, long duration runs (200 h time on stream) were performed under conditions suitable for maximizing H_2 yield, which in view of the results in previous sections are: 600-650 ºC; space time, 0.35 $g_{catalyst}h/g_{EtOH}$, and; S/E molar ratio, 6. A higher S/E ratio was not considered because only a slight increase in H_2 yield would be achieved at the expense of a higher cost for steam generation and product separation (product molar fractions decrease due to dilution).

The evolutions of ethanol conversion and products yield under these conditions are plotted in Figures 11a (600 ºC) and 11b (650 ºC). As observed, intermediate products in the reaction scheme of the process (acetaldehyde and ethylene) are not formed, and the catalyst is highly stable. Thus, ethanol conversion is almost complete (> 0.97) after 200 h time on stream, and there is also a very small variation in products yields. The yield of the carbon products is different at both temperatures due to the opposite effect of temperature on the equilibrium of WGS and methane steam reforming reactions, as previously commented. Thus, the equilibrium of WGS reaction shifts to the left as temperature increases, thus increasing CO

yield and decreasing CO_2 yield, whereas methane steam reforming equilibrium is favored, thus decreasing CH_4 yield. As a consequence of the opposite effect of temperature on the previously mentioned reactions, the H_2 yield remains almost the same at both temperatures.

Figure 11

CONCLUSIONS

The effect operating conditions have on products distribution in the SRE over Ni/La_2O_3-αAl_2O_3 catalysts is complex, as it is a consequence of numerous parallel reactions that are activated by the catalyst, and also due to the contribution of thermal (non catalytic) routes. In the catalytic reforming, these thermal routes have a significant contribution to the extent of some reactions, and therefore to products distribution, i.e., below 600 ºC by means of ethanol dehydrogenation and dehydration and above 600 ºC by ethanol and acetaldehyde decomposition. Furthermore, the WGS reaction, methane steam reforming or direct ethanol steam reforming reactions are not significant in the absence of catalyst, even at high temperature (as revealed by the almost null formation of CO_2 under these conditions).

Temperature notably affects the kinetic behavior of Ni/La_2O_3-αAl_2O_3 catalyst, so that both ethanol conversion and H_2 yield increase considerably with temperature. Acetaldehyde dehydrogenation is the fastest reaction of the kinetic scheme at 500 ºC, and WGS reaction, methane steam reforming and ethanol dehydration are slow reactions, especially the latter. In addition, ethanol dehydration, as well as ethanol and acetaldehyde decomposition reactions, are noticeably enhanced by increasing temperature. The enhancement of methane steam reforming with temperature involves a significant increase in H_2 yield, although this increase is attenuated above 650 ºC because the equilibrium of WGS reaction shifts towards the left at high temperature.

Ethanol conversion and the yields of H_2, CO, CO_2 and CH_4 increase in a very pronounced way by increasing space time to 0.09 $g_{catalyst}h/g_{EtOH}$, whereas those of ethylene and acetaldehyde decrease, because they are primary products in the reaction scheme, i.e., they are formed by the fast reactions of ethanol dehydration and dehydrogenation, respectively. Above 0.09 $g_{catalyst}h/g_{EtOH}$, ethanol conversion is almost complete and products yields do not vary significantly, especially above 600 ºC, as they approach the values corresponding to the thermodynamic equilibrium. The effect of space time is less noticeable at high temperature (650 ºC) due to the significant contribution of thermal routes to the reaction mechanism.

Steam/ethanol (S/E) molar ratio has an important role on conversion and products selectivity. An increase in S/E ratio above the stoichiometric value (3) enhances H_2 selectivity due to the promotion of ethanol and methane steam reforming and WGS reaction, whereas the selectivity to by-products (CO, CH_4, ethylene and acetaldehyde) decreases. Nevertheless, under conditions far from thermodynamic equilibrium (low values of space-time and temperature) ethanol conversion decreases by increasing the S/E ratio above the stoichiometric value due to the attenuation in the rate of some reactions in the kinetic scheme.

In order to maximize H_2 yield, while minimizing by-products formation, the following operating conditions are recommended: 600 ºC, space time above 0.35 $g_{catalyst}h/g_{EtOH}$ and S/E molar ratio = 6. Under these conditions, a H_2 yield of 82% is achieved, which remains constant along 200 h time on stream.

Based on the results, a kinetic scheme has been proposed, which includes the relevant reactions accounting for the products distribution obtained. The reactions of formation/disappearance of acetone or acetic acid are not included in this scheme due to the total absence of these compounds in the products stream in the range of operating conditions studied.

ACKNOWLEDGMENTS

This work has been carried out with financial support from the Ministry of Science and Technology of the Spanish Government and the ERDF Funds (Projects CTQ2012-35263 and CTQ2015-68883-R), the University of the Basque Country (UFI 11/39) and the Basque Government (Project IT748-13). Carolina Montero is grateful for her Ph.D. grants from the National Secretariat of Higher Education, Science, Technology and Innovation of Ecuador SENESCYT (Contract 20110560).

References

[1] International Energy Agency. World Energy Outlook 2016. https:www.aei.org/newsroom/news/2016/november/world-energy-outlook-2016.html.

[2] P. Lanzafame, G. Centi, S. Perathoner, Evolving Scenarios for biorefineries and the impact on catalysis, Catal. Today 234 (2014) 2-12.

[3] P. Mohanty, K.K. Pant, R. Mittal, R. Hydrogen Generation from Biomass Materials: Challenges and Opportunities, in Advances in Bioenergy: The Sustainability Challenge (eds P. D. Lund, J. Byrne, G. Berndes and I. A. Vasalos), John Wiley & Sons, Ltd, Oxford, (2016) pp. 93-108.

[4] A. Hedayati, O. Le Corre, B. Lacarrière, J. Llorca, Dynamic simulation of pure hydrogen production via ethanol steam reforming in a catalytic membrane reactor, Energy 117, Part 2 (2016) 316-324.

[5] D. Li, X. Li, J. Gong, Catalytic reforming of oxygenates: state of the art and future prospects, Chem. Rev. 116 (2016) 11529-11653.

[6] H.B. Aditiya, T.M.I. Mahlia, W.T. Chong, H. Nur, A.H. Sebayang, Second generation bioethanol production: A critical review, Ren. Sust. Energ. Rev. 66 (2016) 631–653.

[7] Y. Sharma, A. Kumar, R. Prasad, S. Upadhyay, Ethanol steam reforming for hydrogen production: Latest and effective catalyst modification strategies to minimize carbonaceous deactivation, Renew. Sus. Ener. Rev., 74 (2017), 89–103.

[8] S. Sun, W. Yan, P. Sun, J. Chen, Thermodynamic analysis of ethanol reforming for hydrogen production, Energy. 44 (2012) 911-924.

[9] M. Ni, D. Leung, M. Leung, A review on reforming bio-ethanol for hydrogen production. Int. J. Hydrog.Energy. 32 (2007) 3238-3247.

[10] J. Vicente, J. Ereña, C. Montero, M.J. Azkoiti, J. Bilbao, A.G. Gayubo, Reaction pathway for ethanol steam reforming on a Ni/SiO_2 catalyst including coke formation. Int. J. Hydrog. Energy. 39 (2014) 18820-18834.

[11] C. Montero, L. Oar-Arteta, A. Remiro, A. Arandia, J. Bilbao, A.G. Gayubo, Thermodynamic comparison between bio-oil and ethanol steam reforming, Int. J. Hydrog. Energy. 40 (2015) 15963-15971.

[12] G. Nahar, V. Dupont, Hydrogen via steam reforming of liquid biofeedstock, Biofuels 3 (2012) 167-91.

[13] J.L. Contreras, J. Salmones, J.A. Colín-Luna, L. Nuño, B. Quintana, I. Córdova, et al., Catalysts for H_2 production using the ethanol steam reforming (a review), Int. J. Hydrog. Energ. 39 (2014) 18835-18853.

[14] A. Kumar, R. Prasad, Y. Sharma, Steam reforming of ethanol: production of renewable hydrogen, Int. J. Environ. Res. Dev. 3 (2014) 203-212.

[15] T. Hou, S. Zhang, Y. Chen, D. Wang, W. Cai, Hydrogen production from ethanol reforming: catalysts and reaction mechanism. Ren. Sust. Energ. Rev. 44 (2015) 132-148.

[16] P. Osorio-Vargas, C.H. Campos, R.M. Navarro, J.L.G. Fierro, P. Reyes, Improved ethanol steam reforming on Rh/Al_2O_3 catalysts doped with CeO_2 or/and La_2O_3: Influence in reaction pathways including coke formation, Appl. Catal. A Gen 505 (2015) 159-172.

[17] P.K. Sharma, N.Saxena, P.K.Roy, A. Bhatt, Hydrogen generation by ethanol steam reforming over Rh/Al_2O_3 and $Rh/CeZrO_2$ catalysts: A comparative study, Int. J. Hydrog. Energ. 41 (2016) 6123-6133.

[18] R. Carrera Cerritos, R. Fuentes Ramírez, A. Aguilera Alvarado, J. Martínez Rosales, T. Viveros García, I. Galindo Esquivel, Steam reforming of ethanol over Ni/Al_2O_3-La_2O_3 catalysts synthesized by sol-gel, Ind. Eng. Chem. Res. 50 (2011) 2576-2584.

[19] R. Trane-Restrup, S. Dahl, A.D. Jensen, Steam reforming of ethanol: Effects of support and additives on Ni-based catalysts. Int. J. Hydrog. Energ. 38 (2013) 15105-15118.

[20] A.F. Lucredio, J.D.A. Bellido, A. Zawadzki, E.M. Assaf, Co catalysts supported on SiO_2 and γ-Al_2O_3 applied to ethanol steam reforming: Effect of the solvent used in the catalyst preparation method. Fuel 90 (2011) 1424-1430.

[21] X. Zhao, G. Lu. Modulating and controlling active species dispersion over Ni-Co bimetallic catalysts for enhancement of hydrogen production of ethanol steam reforming, Int. J. Hydrog. Energ. 41 (2016) 3349-3362.

[22] A. J. Vizcaino, A .Carrero, J. A. Calles, Comparison of ethanol steam reforming using Co and Ni catalysts supported on SBA-15 modified by Ca and Mg. Fuel Process. Technol. 146, (2016) 99-109.

[23] F. Carvalho, Y. Asencios, J. Bellido, E. Assaf, Bio-ethanol steam reforming for hydrogen production over Co_3O_4/CeO_2 catalysts synthesized by one-step polymerization method, Fuel Process. Technol. 142 (2016) 182-191.

[24] S.J. Han, Y. Bang, J. Yoo, J.G. SeoI, K. Song, Hydrogen production by steam reforming of ethanol over mesoporous $Ni–Al_2O_3–ZrO_2$ xerogel catalysts: Effect of nickel content, Int. J. Hydrogen. Energ. 38 (2013) 8285-8292.

[25] A.G. Gayubo., J. Vicente, J. Ereña, C. Montero, M. Olazar, J. Bilbao, Comparison of Ni and Co Catalysts for Ethanol Steam Reformingin a Fluidized Bed Reactor, Catal. Lett. 144 (2014) 1134–1143.

[26] C.K.S. Choong, Z. Zhong, L. Huang, Z. Wang, T.P. Ang, A. Borgna, et al., Effect of calcium addition on catalytic ethanol steam reforming of Ni/Al_2O_3: I. Catalytic stability, electronic properties and coking mechanism, Appl. Catal. A. 407 (2011) 145-154.

[27] K. Elias, A. Lucrédio, E. Assaf, Effect of CaO addition on acid properties of Ni–Ca/Al_2O_3 catalysts applied to ethanol steam reforming, Int. J. Hydrogen. Energ. 38 (2013) 4407-4417.

[28] M.N. Barroso, A.E. Galetti, M.F. Gomez, L.A. Arrúa, M.C. Abello, Ni-catalysts supported on $Zn_xMg_{1-x}Al_2O_4$ for ethanol steam reforming: Influence of the substitution for Mg on catalytic activity and stability, Chem. Eng. J. 222 (2013) 142-149.

[29] G.P. Szijjártó, Z. Pászti, I. Sajó, A. Erdőhelyi, G. Radnóczi, A. Tompos, Nature of the active sites in Ni/$MgAl_2O_4$-based catalysts designed for steam reforming of ethanol, J. Catal. 305 (2013) 290-306.

[30] G. Zeng, R. GuY. Li, The preparation and catalytic behavior of a shell–core Ni/Mg–Al catalyst for ethanol steam reforming, Int. J. Hydrogen. Energ. 38 (2013) 11256-11267.

[31] V. Nichele, M. Signoretto, F. Pinna, F. Menegazzo, I. Rossetti, G. Cruciani, et al., Ni/ZrO_2 catalysts in ethanol steam reforming: Inhibition of coke formation by CaO-doping, Appl. Catal. B. Environm. 150–151 (2014) 12-20.

[32] M.C. Sánchez-Sánchez, R.M. Navarro, J.L.G. Fierro, Ethanol steam reforming over Ni/La–Al_2O_3 catalysts: Influence of lanthanum loading, Catal. Today. 129 (2007) 336-345.

[33] J. Vicente, C. Montero, J. Ereña, M.J. Azkoiti, J. Bilbao A.G. Gayubo., Coke deactivation of Ni and Co catalysts in ethanol steam reforming at mild temperatures in a fluidized bed reactor, Int. J. Hydrogen. Energ. 39 (2014) 12586-12596.

[34] H. Ma, L. Zeng, H. Tian, D. Li, X. Wang, X. Li, et al., Efficient hydrogen production from ethanol steam reforming over La-modified ordered mesoporous Ni-based catalysts, Appl. Catal. B. Environm. 181 (2016) 321-331.

[35] C. Montero, A. Remiro, A. Arandia, P.L. Benito, J. Bilbao, A.G. Gayubo, Reproducible performance of a Ni/La_2O_3-αAl_2O_3 catalyst in ethanol steam reforming under reaction-regeneration cycles, Fuel Process. Technol. 152 (2016) 215-222.

[36] A. Remiro, B. Valle, A.T. Aguayo, J. Bilbao, A.G. Gayubo, Operating conditions for attenuating Ni/La_2O_3–αAl_2O_3 catalyst deactivation in the steam reforming of bio-oil aqueous fraction, Fuel. Process. Technol. 115 (2013) 222-232.

[37] J. Mazumder, H. I. de Lasa. Fluidizable La_2O_3 promoted Ni/γ-Al_2O_3 catalyst for steam gasification of biomass: Effect of catalyst preparation conditions, Appl. Catal. B Environm. 168–169 (2015) 250–265.

[38] M. Sugisawa, K. Takanabe, M. Harada, J. Kubota, K. Domen, Effects of La addition to Ni/Al_2O_3 catalysts on rates and carbon deposition during steam reforming of n-dodecane, Fuel. Process. Technol. 92 (2011) 21–25

[39] C. Li, Y. Chen, Temperature-programmed-reduction studies of nickel oxide/alumina catalysts: effects of the preparation method, Thermochim. Acta 256 (1995) 457-465

[40] B. Valle, B. Aramburu, A. Remiro, J. Bilbao, A.G. Gayubo, Effect of calcination/reduction conditions of Ni/La_2O_3–αAl_2O_3 catalyst on its activity and stability for hydrogen production by steam reforming of raw bio-oil/ethanol, Appl. Catal. B Environm. 147 (2014) 402-410.

[41] C. Montero, A. Ochoa, P. Castaño, J. Bilbao, A.G. Gayubo, Monitoring Ni^0 and coke evolution during the deactivation of a Ni/La_2O_3–αAl_2O_3 catalyst in ethanol steam reforming in a fluidized bed, J. Catal. 331 (2015) 181-192.

[42] A.N. Fatsikostas, X.E. Verykios, Reaction network of steam reforming of ethanol over Ni-based catalysts, J. Catal. 225 (2004) 439-452

[43] C. Melchor-Hernández, A. Gómez-Cortés, G. Díaz, Hydrogen production by steam reforming of ethanol over nickel supported on La-modified alumina catalysts prepared by sol–gel, Fuel. 107 (2013) 828-835.

620 [44] L. Barattini, G. Ramis, C. Resini, G. Busca, M. Sisani, U. Costantino, Reaction path of
621 ethanol and acetic acid steam reforming over Ni–Zn–Al catalysts. Flow reactor studies,
622 Chem. Eng. J. 153 (2009) 43-49.

623 [45] A.N. Fatsikostas, D.I. Kondarides, X.E. Verykios, Production of hydrogen for fuel cells
624 by reformation of biomass-derived ethanol, Catal. Today. 75 (2002) 145-155.

625 [46] I. Llera, V. Mas, M.L. Bergamini, M. Laborde, N. Amadeo, Bio-ethanol steam
626 reforming on Ni based catalyst. Kinetic study, Chem. Eng. Sci. 71 (2012) 356-366.

627 [47] M. Patel, T. Jindal, K. Pant. Kinetic study of steam reforming of ethanol on Ni-based
628 ceria-zirconia catalyst, Ind. Eng. Chem. Res. 52 (2013) 15763-15771

629 [48] C. Zhang, S. Li, G. Wu, Z. Huang, Z. Han, T. Wang, et al., Steam reforming of ethanol
630 over skeletal Ni-based catalysts: A temperature programmed desorption and kinetic
631 study, AIChE J. 60 (2014) 635-644.

632 [49] M. Dan, L. Senila, M. Roman, M. Mihet, M.D. Lazar, From wood wastes to hydrogen –
633 Preparation and catalytic steam reforming of crude bio-ethanol obtained from fire wood,
634 Renew. Energ. 74 (2015) 27-36.

635 [50] Y. Wu, J.C. Santos, P. Li, J.-. Yu, A.F. Cunha, A.E. Rodrigues, Simplified kinetic
636 model for steam reforming of ethanol on a Ni/Al_2O_3 catalyst, Can. J. Chem. Eng. 92
637 (2014) 116-130.

638 [51] P.D. Vaidya, A.E. Rodrigues, Insight into steam reforming of ethanol to produce
639 hydrogen for fuel cells, Chem. Eng. J. 117 (2006) 39-49.

640 [52] B. Banach, A. Machocki, P. Rybak, A. Denis, W. Grzegorczyk, W. Gac, Selective
641 production of hydrogen by steam reforming of bio-ethanol, Catal. Today. 176 (2011)
642 28-35.

643 [53] S. Li, M. Li, C. Zhang, S. Wang, X. Ma, J. Gong, Steam reforming of ethanol over
644 Ni/ZrO_2 catalysts: Effect of support on product distribution, Int. J. Hydrogen. Energ. 37
645 (2012) 2940-2949.

646

647

648

649

650 **Table 1.** Physical and chemical properties of $Ni/La_2O_3–\alpha Al_2O_3$ catalyst.

Technique	Property	Results
N_2 Physisorption	S_{BET} (m^2/g)	35
ICP	Ni (%)	8.8
	La (%)	6.8
H_2 Chemisorption	Metal Dispersion (%)	4.7
	Metal active Surface (m^2/g)	3.1
XRD	Crystal size (Å), 2θ =52º	106

651

652

FIGURE CAPTIONS

Figure 1. Molar fractions (dry basis) of ethanol (a) and H_2 (b) obtained in runs without catalyst at different temperatures and S/E molar ratios.

Figure 2. Molar fractions (dry basis) of acetaldehyde (a), ethylene (b), CO (c) and CH_4 (d) obtained in runs without catalyst at different temperatures and S/E molar ratios.

Figure 3. Effect of temperature on ethanol conversion and H_2 yield in the SRE process over $Ni/La_2O_3–\alpha Al_2O_3$ catalyst for two values of space time. S/E molar ratio =3.-

Figure 4. Effect of temperature on carbon products yields in the SRE process over $Ni/La_2O_3–\alpha Al_2O_3$ catalyst with a space time of 0.04 $g_{catalyst}h/g_{EtOH}$ (a) and 0.35 $g_{catalyst}h/g_{EtOH}$ (b). S/E molar ratio =3.

Figure 5. Effect of space time on ethanol conversion and H_2 yield in the SRE process over $Ni/La_2O_3–\alpha Al_2O_3$ catalyst at different temperatures. S/E molar ratio =3.

Figure 6. Effect of space time on carbon products yield in the SRE process over $Ni/La_2O_3–\alpha Al_2O_3$ catalyst at 500 ºC (a) and 650 (b) ºC. S/E molar ratio =3.

Figure 7. Effect of S/E molar ratio on ethanol conversion and H_2 yield in the SRE process over $Ni/La_2O_3–\alpha Al_2O_3$ at 600 ºC and space time of 0.18 $g_{catalyst}h/g_{EtOH}$.-

Figure 8. Effect of S/E molar ratio on carbon products selectivity in the SRE process over $Ni/La_2O_3–\alpha Al_2O_3$ at 600 ºC and space time of 0.18 $g_{catalyst}h/g_{EtOH}$.-

Figure 9. Effect of temperature on ethanol conversion and H_2 yield in the SRE process over $Ni/La_2O_3–\alpha Al_2O_3$ for two different S/E molar ratios. Space time of 0.04 $g_{catalyst}h/g_{EtOH}$.

Figure 10. Kinetic scheme proposed for the SRE process over $Ni/La_2O_3–\alpha Al_2O_3$ catalyst.

Figure 11. Evolution with time on stream of ethanol conversion and products yield in the SRE process over $Ni/La_2O_3–\alpha Al_2O_3$ at 600 ºC (a) and 650 ºC (b) for 0.35 $g_{catalyst}h/g_{EtOH}$ and S/E molar ratio = 6.

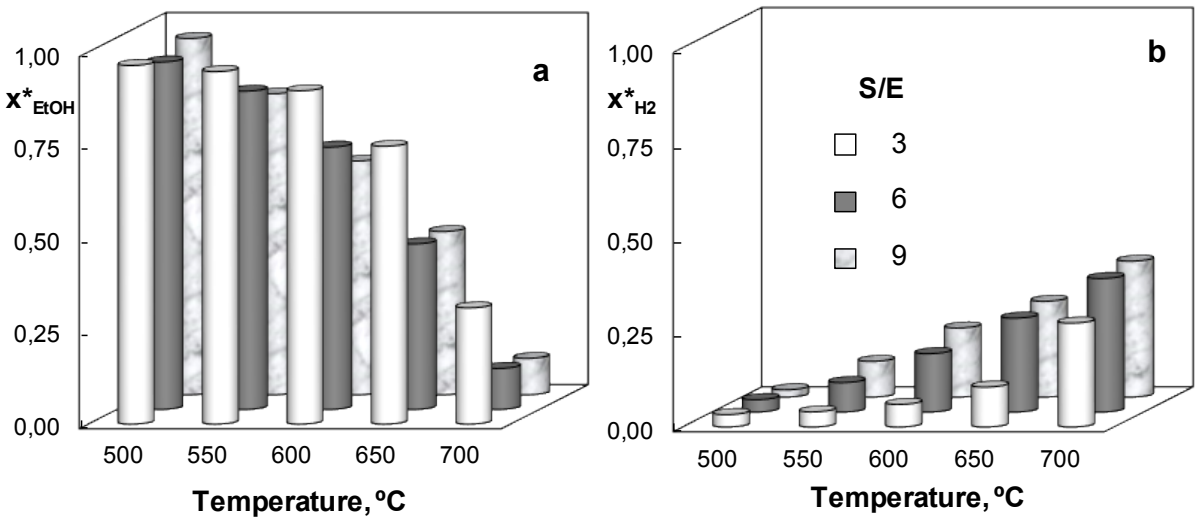

Figure 1

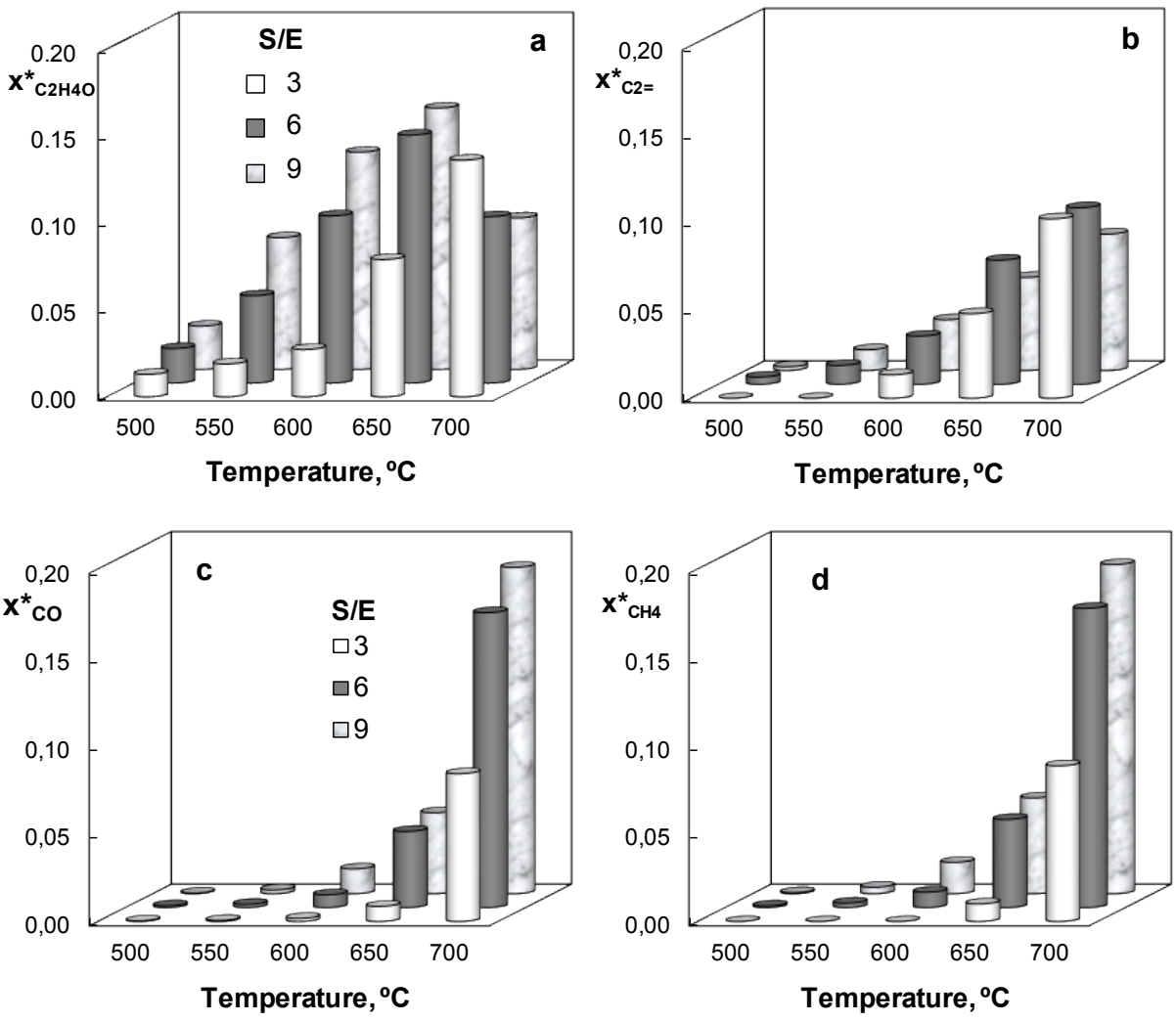

Figure 2

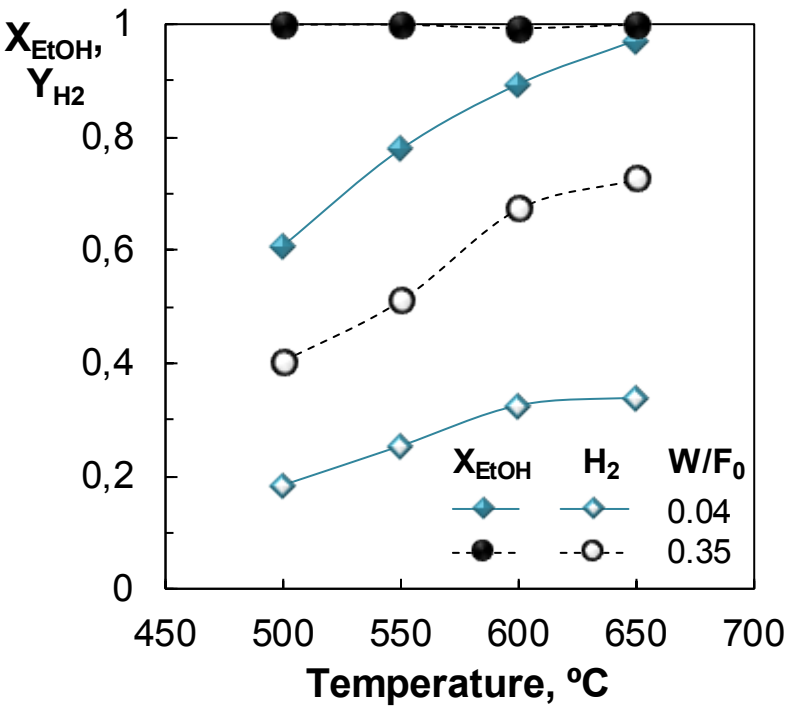
X_EtOH, Y_H2
1
0,8
0,6
0,4
0,2
0
450
500
550
600
650
700
Temperature, ºC
X_EtOH
H_2
W/F_0
0.04
0.35

Figure 3

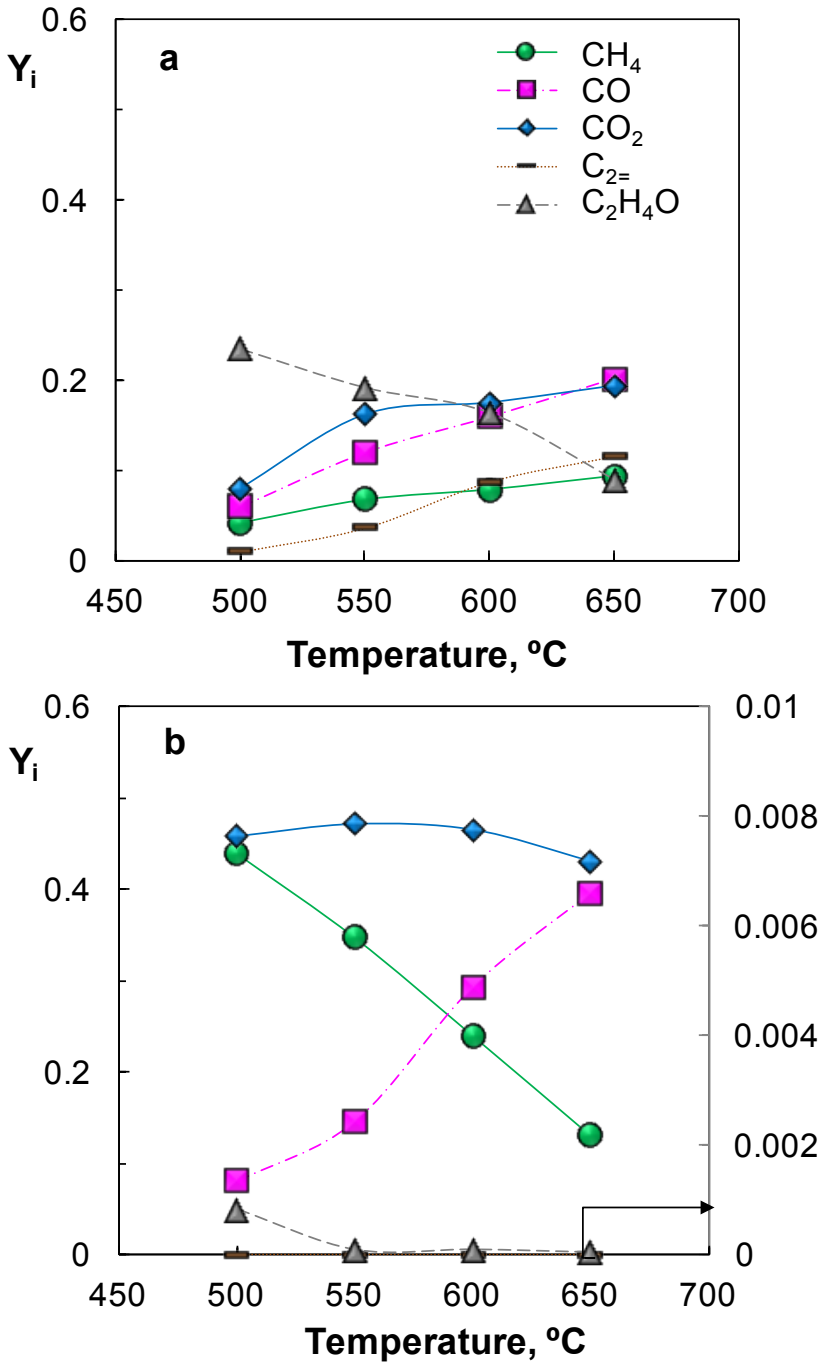
a
Y_i
0.6
0.4
0.2
0
CH_4
CO
CO_2
$C_{2=}$
C_2H_4O
450
500
550
600
650
700
Temperature, ºC
b
Y_i
0.6
0.4
0.2
0
0.01
0.008
0.006
0.004
0.002
0
450
500
550
600
650
700
Temperature, ºC

Figure 4

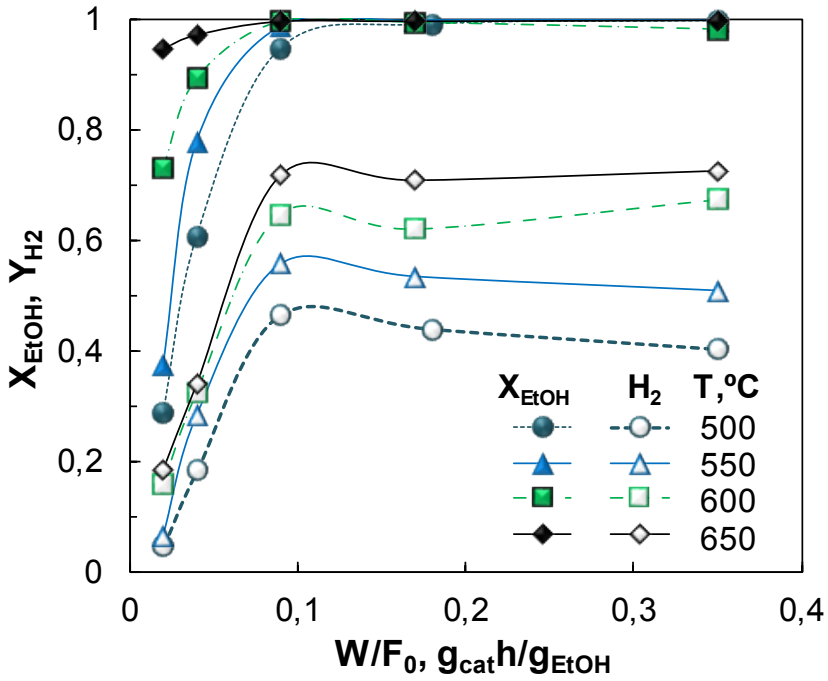
1
0,8
0,6
0,4
0,2
0
0
0,1
0,2
0,3
0,4
X_EtOH, Y_H2
W/F_0, g_cat h/g_EtOH
X_EtOH
H_2
T,°C
500
550
600
650

Figure 5

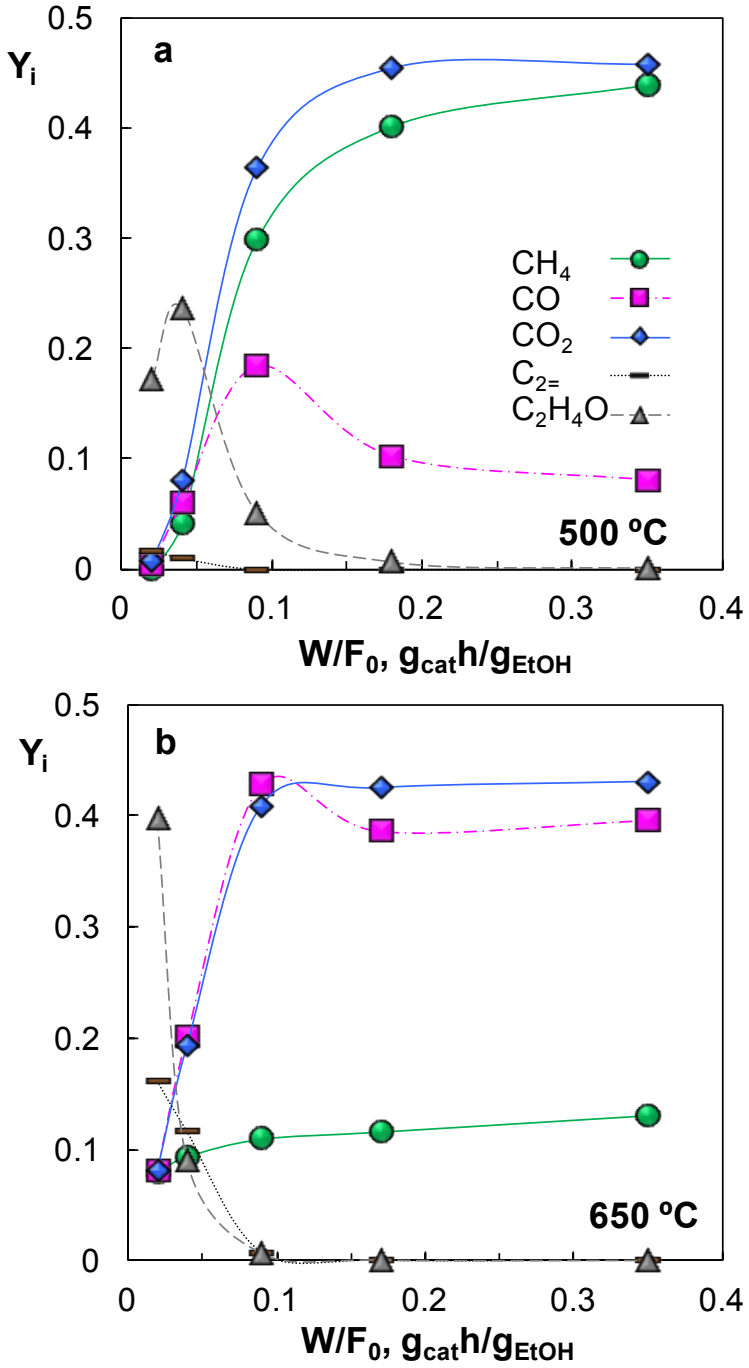
a
b
Y_i
CH_4
CO
CO_2
$C_{2=}$
C_2H_4O
500 ºC
650 ºC
W/F_0, $g_{cat}h/g_{EtOH}$
0
0.1
0.2
0.3
0.4
0.5

Figure 6

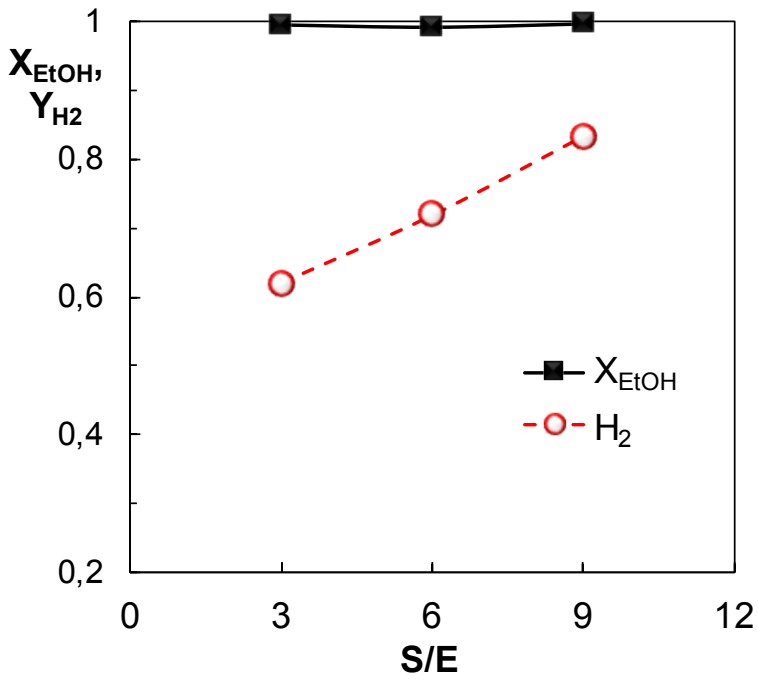

Figure 7

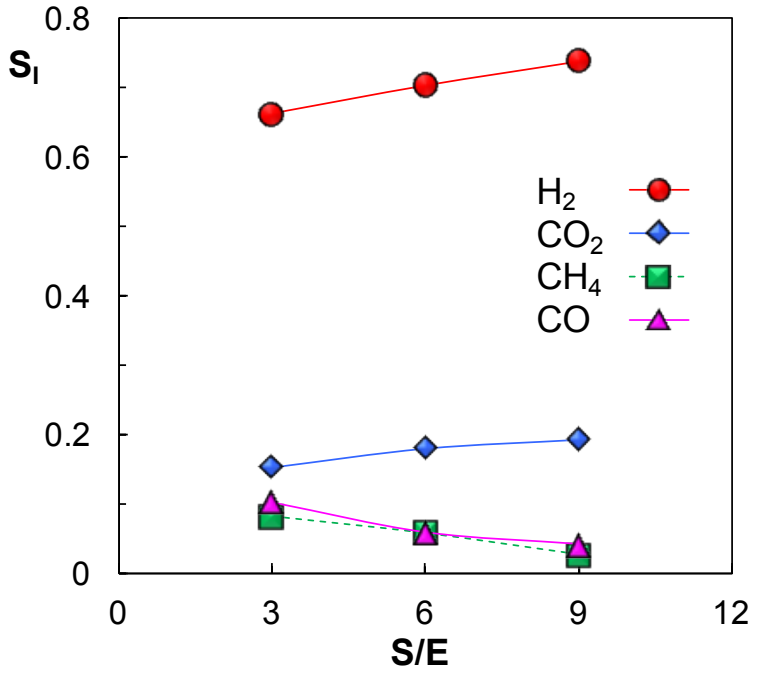

Figure 8

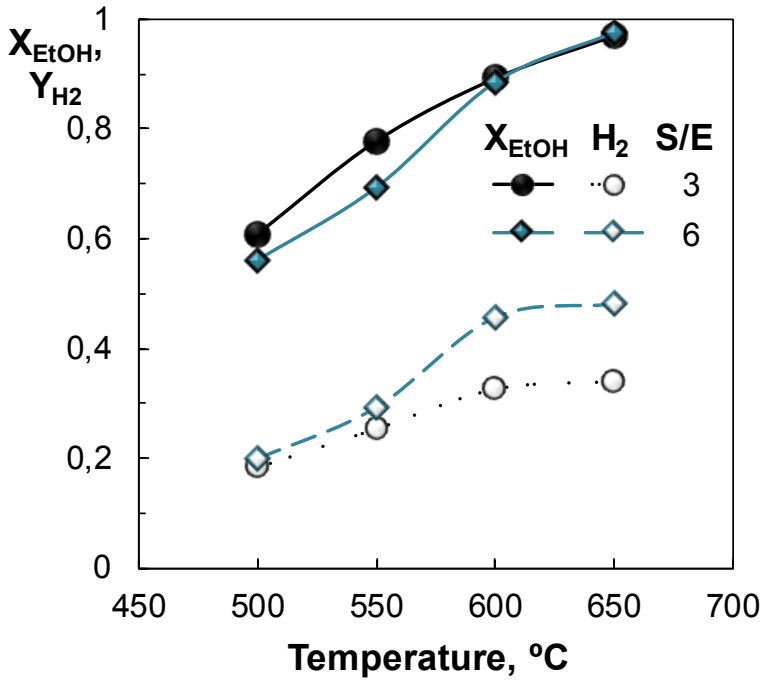
X_EtOH, Y_H2
1
0,8
0,6
0,4
0,2
0
450
500
550
600
650
700
Temperature, ºC
X_EtOH
H_2
S/E
3
6

Figure 9

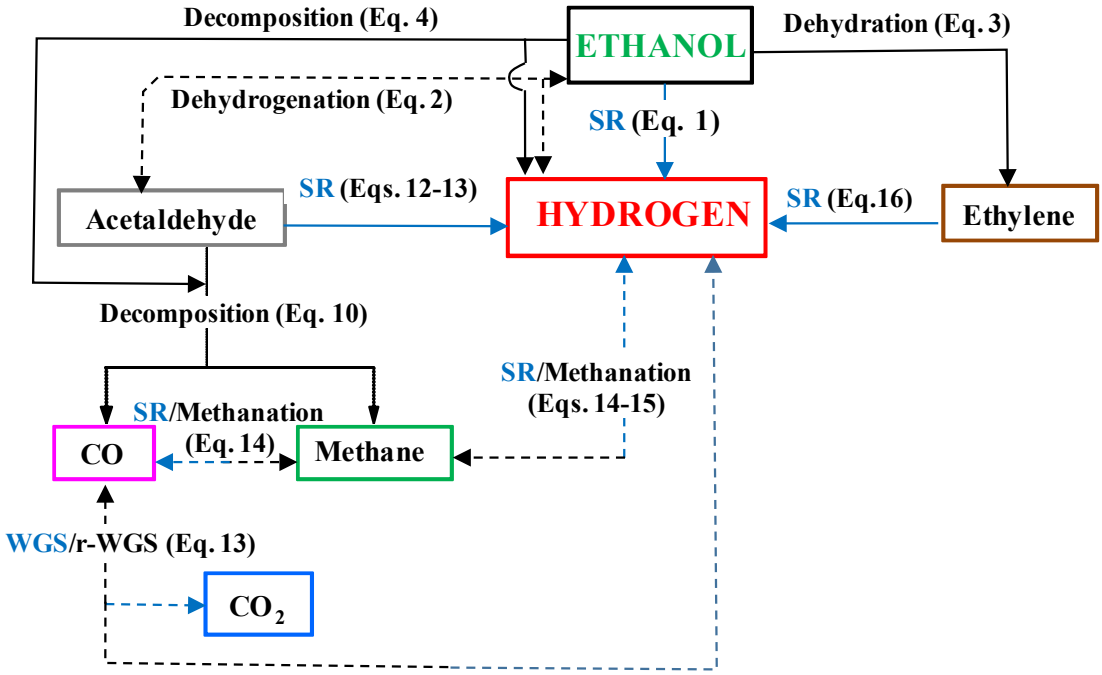
Decomposition (Eq. 4)
ETHANOL
Dehydration (Eq. 3)
Dehydrogenation (Eq. 2)
SR (Eq. 1)
Acetaldehyde
SR (Eqs. 12-13)
HYDROGEN
SR (Eq.16)
Ethylene
Decomposition (Eq. 10)
SR/Methanation
(Eqs. 14-15)
SR/Methanation
(Eq. 14)
CO
Methane
WGS/r-WGS (Eq. 13)
CO2

Figure 10

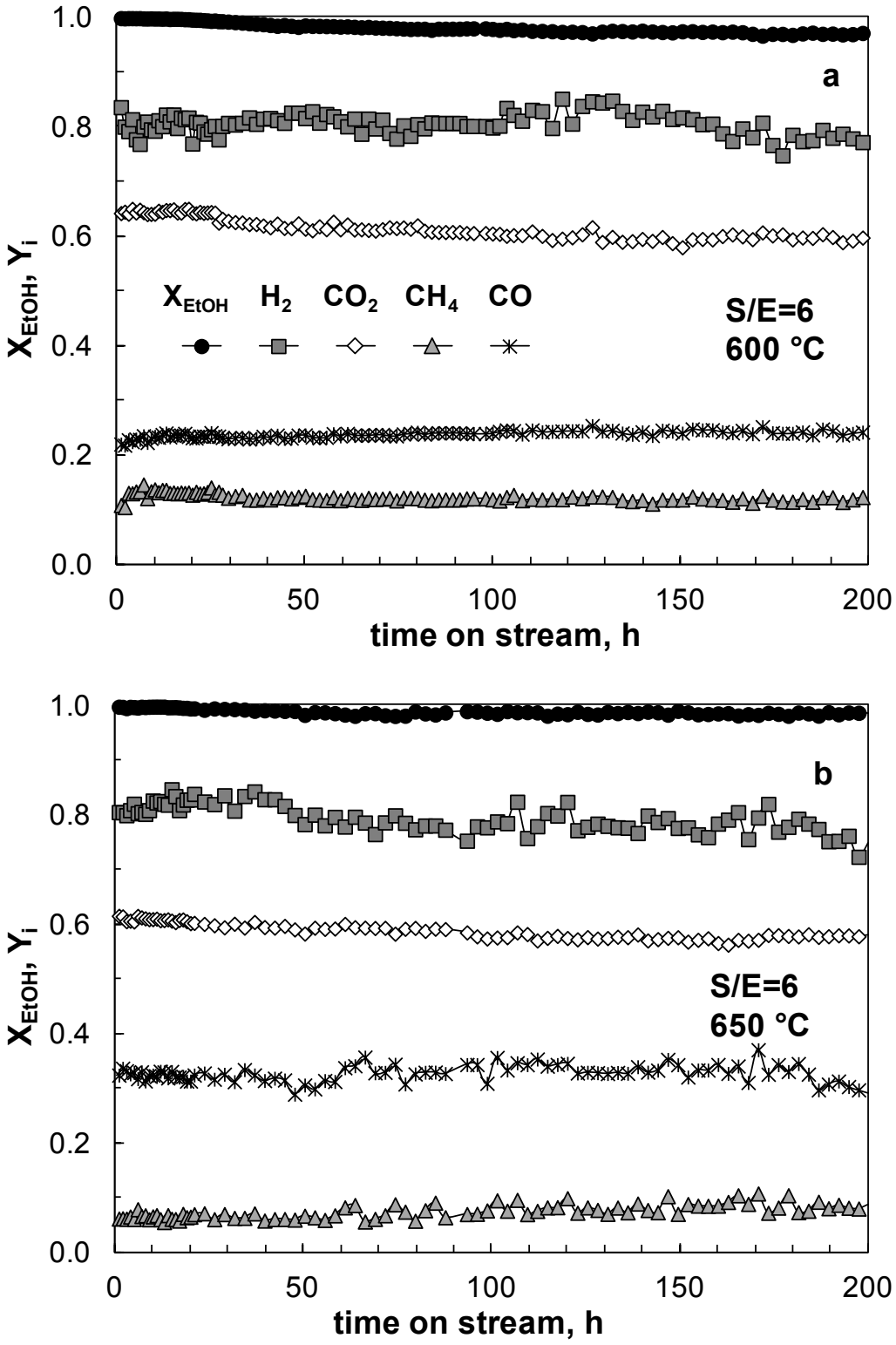
a
b
X_{EtOH}
H_2
CO_2
CH_4
CO
S/E=6
600 °C
650 °C
X_{EtOH}, Y_i
time on stream, h
0.0
0.2
0.4
0.6
0.8
1.0
0
50
100
150
200

Figure 11